bioRxiv preprint doi: https://doi.org/10.1101/415927; this version posted September 13, 2018. The copyright holder for this preprint (which was not certified by peer review) is the author/funder. All rights reserved. No reuse allowed without permission.

A yeast model of calcium-responsive transactivator protein (CREST) proteinopathy shows that PBP1/ATXN2 modifies CREST aggregation and toxicity.

By Sangeun Park, Sei-Kyoung Park and Susan W. Liebman*

Department of Pharmacology, U. of Nevada, Reno

bioRxiv preprint doi: https://doi.org/10.1101/415927; this version posted September 13, 2018. The copyright holder for this preprint (which was not certified by peer review) is the author/funder. All rights reserved. No reuse allowed without permission.

Abstract

Proteins encoded by genes that cause familial neurodegenerative disease often form insoluble amyloid-like aggregates in diseased patients' neurons. Several such proteins, e.g. TDP-43, aggregate and are toxic when expressed in yeast. Finding that deletion of the ATXN2 ortholog, *PBP1,* reduced yeast TDP-43 toxicity, lead to discoveries that ATXN2 is an amyotrophic lateral sclerosis (ALS) risk factor and that lowered ATXN2 levels are therapeutic in a mouse ALS model. Likewise, new yeast neurodegenerative disease models could allow identification of disease risk factors and provide a drug discovery platform. Mutations in *SS18L1,* which encodes CREST, are associated with ALS. CREST, a chromatin-remodeling factor, contains an aggregation prone domain. Here, we show that CREST is toxic in yeast and inhibits silencing of telomerically located genes. Toxicity is enhanced by the [PIN^{+}] prion and reduced by deletion of *PBP1/ATXN2.* CREST forms nuclear and occasionally cytoplasmic foci that stain with an amyloid dye. Overexpression of PBP1 caused considerable CREST co-localization with PBP1 tagged cytoplasmic granules which might promote toxic aggregation of CREST. These results extend the spectrum of ALS associated proteins affected by *PBP1/ATXN2*, supporting the hypothesis that therapies targeting ATXN2 may be effective for a wide range of neurodegenerative diseases.

bioRxiv preprint doi: https://doi.org/10.1101/415927; this version posted September 13, 2018. The copyright holder for this preprint (which was not certified by peer review) is the author/funder. All rights reserved. No reuse allowed without permission.

Introduction

Mutations in an increasing number of human genes have been found to cause familial neurodegenerative disease [1,2]. Proteins encoded by these genes are often soluble in healthy individuals, but form insoluble amyloid-like aggregates that seed further aggregation in the neurons of patients with disease. For example, such conformational changes have been seen for: Aβ, associated with Alzheimer's disease; α-synuclein with Parkinson's disease; TDP-43, FUS and others with amyotrophic lateral sclerosis (ALS) and frontotemporal dementia (FTD); and huntingtin with Huntington's disease. Wild-type and mutant forms of these proteins, are respectively associated with aggregates in sporadic and familial forms of the diseases. Overexpression of either wild-type or mutant causes toxicity, although the mutant forms are often toxic at lower concentrations than the wild-type[3].

Conformational change of several yeast proteins from a soluble conformation to insoluble self-seeding aggregates, called prions, causes transmissible phenotypic changes [4-15]. Furthermore, the presence of one prion aggregate enhances the *de novo* appearance of heterologous prions. For example, the endogenous yeast prion [*PIN*$^+$], which is an amyloid form of the RNQ1 protein, promotes the *de novo* aggregation of the SUP35 protein to form the [*PSI*$^+$] prion. This could occur by cross-seeding or by sequestration of proteins such as chaperones by the amyloid [*PIN*$^+$] prion[8,16-25].

Yeast has proved to be useful in the study of disease-specific proteins that form prion-like aggregates[26-33]. When human proteins associated with aggregation in neurodegenerative disease were expressed in yeast, they formed aggregates and caused toxicity. Curiously the toxicity of several of these proteins, e.g. TDP-43, FUS or huntingtin, is enhanced by the presence of the [*PIN*$^+$] prion[26,34,35]. These yeast models have allowed the identification of yeast genes that either alter the disease protein's aggregation or enhance or reduce its toxicity. Remarkably, human homologs of these yeast modifier genes have confirmed (*PICALM* for Alzheimer's [36-38], *PARK9* for Parkinson [36,39]), and identified new

bioRxiv preprint doi: https://doi.org/10.1101/415927; this version posted September 13, 2018. The copyright holder for this preprint (which was not certified by peer review) is the author/funder. All rights reserved. No reuse allowed without permission.

(*ATXN2* [40-44] for ALS and *XPO1*, *ADSSL1* and *RABGEF1* for Alzheimer's [36,38]), human risk factors for the modeled disease. Indeed, the discovery in yeast that deletion of the *ATXN2* (Ataxin-2) ortholog, *PBP1,* reduced TDP-43 toxicity, lead to the recent exciting findings that reduction in ATXN2 levels moderates neurotoxicity in ALS mouse models[41]. Thus the establishment of new yeast neurodegenerative disease models may lead to the identification of new risk factors for human disease as well as provide a screening platform for drug discovery.

Recently, mutations in *SS18L1* have been shown to cause ALS [45,46]. *SS18L1* encodes the calcium-responsive transactivator (CREST) protein which is an essential component of the nBAF neuron-specific chromatin remodeling complex and is related to the yeast SWI/SNF chromatin remodeling complex[47-49]. Overexpression of CREST inhibits neurite outgrowth in cultured neurons and causes retina degeneration in transgenic Drosophila[46,50]. Also, CREST co-immunoprecipitates with FUS in neuron lysates[46,50]. In cultured cells, transformed CREST forms predominantly nuclear dots with some cytoplasmic foci. Also like other ALS associated proteins, CREST is recruited to stress-induced ribonucleoprotein particle (RNP) granules[50,51]. RNP proteins must reversibly aggregate in granules as part of their normal cellular function, but this ability to aggregate could lead to the formation of pathological aggregates. Indeed, TDP-43 and FUS have prion-like domains and have been found in cytoplasmic aggregates in the neurons of patients with ALS. While no such patient aggregates have yet been reported for CREST, it has an unstructured prion-like domain predicted to form amyloid-like aggregates[46]. In a fly model with overexpressed CREST, it forms nuclear dots that do not overlap paraspeckles. CREST in cell culture was slightly resistant to triton-X but was solubilized by SDS[50].

Here, we establish a new ALS model in yeast. We show that the CREST human chromatin remodeling complex component and transcriptional activator is toxic and forms amyloid when expressed in yeast. Furthermore, CREST, inhibits genomic silencing at telomeric regions thereby enhancing flocculation

bioRxiv preprint doi: https://doi.org/10.1101/415927; this version posted September 13, 2018. The copyright holder for this preprint (which was not certified by peer review) is the author/funder. All rights reserved. No reuse allowed without permission.

(cell clumping). CREST toxicity is increased by the endogenous yeast [*PIN*$^+$] prion. Deletion of *PBP1* reduces CREST toxicity while increasing flocculation. The enhanced flocculation is likely caused by increased CREST cellular transcriptional activation function. CREST is largely nuclear, but also forms some cytoplasmic foci. Upon overexpression of *PBP1*, a large portion of CREST leaves the nucleus and co-localizes with PBP1 tagged cytoplasmic granules.

Results

Expression of human CREST in yeast is toxic.

Growth of yeast expressing fusions of human CREST cDNA and GFP from a *GAL* promoter on *CEN*, 2μ and integrating vectors was compared with yeast transformed with control *GAL-GFP* vectors (Fig. 1abc). Expression of the *GAL* controlled genes was turned on with a constitutively expressed fusion of the human estrogen receptor hormone-binding domain, the yeast *GAL4* DNA-binding domain and the VP16 viral transcriptional activator, which was activated by the addition of β-estradiol. The high level of β-estradiol used here (1μM) in glucose media results in more expression from the *GAL* promoter than that obtained by traditional induction on 2% galactose without β-estradiol[52]. Growth inhibition is evident but slight when CREST-GFP was expressed from a CEN vector (Fig. 1a) and more inhibition is seen when 2μ (Fig. 1b) or integrating vectors (Fig. 1c) were used.

Since the presence of the [*PIN*$^+$] prion causes enhanced toxicity of the human genes huntingtin/polyQ, TDP-43 and FUS[26,34,35,53] , we asked if [*PIN*$^+$] would likewise increase toxicity of CREST and found that it did (Fig. 1d and Supplementary Fig. 2).

Expression of human CREST causes yeast flocculation and reduces telomeric silencing.

While working with *GAL-CREST-GFP* and *GAL-GFP* transformants we noticed that expression of CREST-GFP caused cells in liquid culture to settle very rapidly compared to the GFP controls. In a measured

bioRxiv preprint doi: https://doi.org/10.1101/415927; this version posted September 13, 2018. The copyright holder for this preprint (which was not certified by peer review) is the author/funder. All rights reserved. No reuse allowed without permission.

experiment we found that overexpression of CREST caused flocculation, while overexpression of TDP-43 or FUS did not (Fig. 2a).

Since CREST increased flocculence in yeast we searched the database for deletions of endogenous yeast genes that likewise increase flocculence. Four of the genes found, *SDC1, SPP1, SWD1* and *SWD3* are components of the COMPASS complex that is required to silence genes located in telomeric regions[54]. When COMPASS silencing is eliminated, *FLO* genes, which are located in telomeric regions, are activated and flocculation occurs [55,56]. Thus we hypothesized that expression of the human chromatin remodeling CREST protein in yeast modifies chromatin structure causing a release of silencing of telomerically located genes including the *FLO* genes, resulting in flocculation.

To test this hypothesis we examined the effect of CREST expression on the activity of a silenced *URA3* yeast gene in a strain (UCC3537) that is mutant for *URA3* at the normal locus, but carries a wild-type *URA3* gene copy inserted into the truncated left arm of chromosome VII near the telomere [57,58]. Because of the proximity of the telomere, the wild-type *URA3* gene is silenced in some of the cells. This silencing is easily detected because it results in a culture with a mixture of cells some expressing and some not expressing *URA3.* This allows the culture to grow both on media lacking uracil and on media containing 5-FOA that poisons cells expressing *URA3:* cells in the culture that are Ura3$^+$ grow on the uracil-less medium, while the Ura3$^-$ cells in the culture grow 5-FOA media. This is unlike cultures with all cells expressing *URA3* which can grow on uracil-less media but not on 5-FOA media. It is also unlike cultures of all Ura3$^-$ cells that can grow on 5-FOA media, but not on uracil-less medium. For a control we used a deletion of *RAD6* which reduces the silencing of *URA3* in this assay and is seen as a reduction in growth on 5-FOA medium[58].

bioRxiv preprint doi: https://doi.org/10.1101/415927; this version posted September 13, 2018. The copyright holder for this preprint (which was not certified by peer review) is the author/funder. All rights reserved. No reuse allowed without permission.

We induced CREST from *GAL1-CREST* transformants by spotting on galactose media. It was critical for our assay that this lower level of CREST induction, compared to using estradiol as above, did not inhibit growth (see +Ura spots in Fig. 2c). Therefore, the finding that CREST induction inhibited growth on galactose +FOA medium (Fig. 2c) is significant and indicates a reduction in silencing of the telomeric *URA3* gene. This reduced silencing makes more cells Ura+ and therefore unable to grow on +5-FOA. It is noteworthy that we can detect an effect on silencing even at a level of CREST expression that is not toxic, and we speculate that more inhibition of silencing likely occurs when CREST is expressed at higher levels.

CREST forms largely nuclear amyloid dots but also some cytoplasmic amyloid foci.

CREST-GFP expressed in yeast was localized to nuclear dots. This occurred similarly in [*PIN*$^{+}$] and [*pin*$^{-}$] cells. CREST-GFP dots were largely clustered in nuclei but smaller cytoplasmic foci were also visible especially after longer induction times (Fig. 3a). Nuclear localization was confirmed by using a constitutively expressed nuclear HTB1-mCh marker (Fig. 3b) which co-localized with CREST-GFP. CREST foci also stained with the amyloid dye thioflavin T (Fig. 3c). For controls we show TDP-43 and FUS aggregates that respectively do not and do stain with Thioflavin T[59].

PBP1 affects the aggregation, toxicity and functionality of CREST.

Overexpression of yeast's *PBP1*, a homolog of human *ATXN2*, enhances, while *PBP1* deletion reduces, the toxicity of TDP-43 expressed in yeast[40]. This led to the discovery that ATXN2 intermediate-length polyglutamine expansions, which are associated with increased ATXN2 protein levels, are a risk factor for ALS [40]. Work in a variety of model organisms including mice now suggests that *ATXN2* is a modifier of many neurodegenerative diseases[41].

bioRxiv preprint doi: https://doi.org/10.1101/415927; this version posted September 13, 2018. The copyright holder for this preprint (which was not certified by peer review) is the author/funder. All rights reserved. No reuse allowed without permission.

We thus tested the effect of overexpressing *PBP1* on the aggregation and toxicity of CREST in yeast. We found a dramatic increase in cytoplasmic CREST dots when *PBP1* was overexpressed Fig. 4a. This was not due to an increase in CREST protein level (Fig. 4b). We also found the CREST-DsRed dots co-localized with PBP1-GFP tagged cytoplasmic granules (Fig. 4c). Surprisingly staining of CREST foci with thioflavin T was dramatically reduced in cells overexpressing PBP1 (Fig. 3c).

Overexpression of *PBP1* itself was toxic in our system (Fig. 4e) so the effect on CREST toxicity could not be determined. However, we clearly show that deletion of *PBP1* reduced toxicity in either a [PIN^+] or [pin^-] background (Fig. 4d and Supplemental Fig. 2) and enhanced flocculation (Fig. 2b**)** caused by CREST without reducing the level of CREST expressed (Fig. 4b). We could not detect any difference in the cellular location CREST due to deletion of *PBP1.*

Unlike [PIN^+] aggregates, CREST dots and foci do not seed SUP35 prion formation.

Considerable evidence suggests that amyloid-like aggregates of one protein can facilitate the *de novo* aggregation of certain heterologous proteins. Such a phenomenon could be an important risk factor for disease. While there are no yeast proteins that are homologous to the human CREST, the yeast protein with the most similarity to CREST, using a BLAST search, is RNQ1, the component of [PIN^+]. Thus, we asked if aggregates of CREST, like [PIN^+] aggregates, could facilitate the *de novo* aggregation of SUP35 to form the [PSI^+] prion. In [PIN^+] but not [pin^-] cells, transient overexpression of SUP35NM-GFP causes the appearance of large fluorescent SUP35NM-GFP rings and converts [psi^-] cells into [PSI^+] [8,17,52,60]. Here we detect conversion into [PSI^+], which causes readthrough of nonsense codons, by the appearance of adenine protrophy despite the presence of the nonsense mutation *ade1-14.* We found that unlike [PIN^+], or overexpression of a variety of QN-rich yeast proteins [8], overexpression of CREST did not cause the appearance of fluorescent SUP35NM-GFP rings or of adenine prototrophy (Fig. 5).

bioRxiv preprint doi: https://doi.org/10.1101/415927; this version posted September 13, 2018. The copyright holder for this preprint (which was not certified by peer review) is the author/funder. All rights reserved. No reuse allowed without permission.

Cytoplasmic aggregates of CREST appear during heat stress and disappear following stress.

When CREST is expressed in yeast for 5-6 hrs most of the protein is found in nuclear dots with just occasional cytoplasmic foci (see Fig. 3 and Fig. 6 left). However, when cells with nuclear CREST are stressed by incubation at high temperature there is a dramatic increase in the appearance of cytoplasmic foci (Fig. 6 middle) that partially co-localize with an EDC3-mCh P-body marker. Following a return to 30°C, cytoplasmic CREST aggregates disappear along with P-bodies.

Discussion

Our data show that human CREST expressed in yeast shares four properties with other ALS associated proteins: 1) formation of amyloid foci; 2) toxicity enhanced by the yeast prion [*PIN*$^+$]; 3) toxicity reduced by deletion of *PBP1*; 4) association with RNP cytoplasmic granules.

We first described [*PIN*$^+$], the prion form of the RNQ1 protein, because its presence allowed the efficient conversion of the SUP35 protein to its prion form, [*PSI*$^+$][8,17,61]. It was later shown that [*PIN*$^+$] is also required for the efficient aggregation and toxicity of polyQ in yeast[26]. The mechanisms causing these effects is still unknown. Some data support the hypothesis that the [*PIN*$^+$] aggregates of RNQ1 cross-seed aggregation of heterologous proteins such as SUP35 and polyQ. Likewise some, but not all evidence suggests that the [*PIN*$^+$] aggregates bind proteins such as chaperones that would otherwise inhibit aggregation of the heterologous SUP35 or polyQ protein, thereby enhancing their aggregation[18-25].

We recently showed that toxicity of TDP-43 and FUS is enhanced by the presence of [*PIN*$^+$][35,53]. Both of these proteins contain Q/N-rich regions and co-aggregate with polyQ disease protein alleles of huntingtin[62,63]. Surprisingly, we did not detect an effect of [*PIN*$^+$] on TDP-43 or FUS aggregation. Likewise, CREST is a Q-rich protein. We show here that the toxicity of CREST is enhanced by [*PIN*$^+$],

bioRxiv preprint doi: https://doi.org/10.1101/415927; this version posted September 13, 2018. The copyright holder for this preprint (which was not certified by peer review) is the author/funder. All rights reserved. No reuse allowed without permission.

again with no detectable effect on aggregation. Apparently the toxicity of the aggregates is altered without a change in their appearance. A recent finding that deletion of PBP1 causes a reduction in the level of RNQ1 protein[64] could have explained the reduced CREST, TDP-43 and FUS toxicity seen in *pbp1Δ* cells if the lowered RNQ1 level reduced the potency of [*PIN*$^+$]. However, we show here that this is not the case because *pbp1Δ* reduces CREST toxicity even in the absence of [*PIN*$^+$].

We have shown that the presence of certain QN-rich aggregates can substitute for [*PIN*$^+$] and allow the efficient induction of [*PSI*$^+$] by overexpression of SUP35[8]. This fact, plus the observation that RNQ1, the [*PIN*$^+$] prion protein, is the most homologous yeast protein to CREST, prompted us to ask if overexpression of CREST could substitute for [*PIN*$^+$]. However, CREST did not provide any [*PIN*$^+$] activity. Possibly the level of CREST in cytoplasmic foci is insufficient for this activity.

Curiously heterologous prion aggregates not only enhance *de novo* formation of a prion but they also promote the loss of heterologous prion aggregates. One mechanism for this has been shown to be titration of chaperones needed for prion propagation[24]. Likewise, CREST has been shown to suppress polyQ-mediated huntingtin aggregation and toxicity [65].

Many of the ALS associated proteins, e.g. TDP-43, FUS and TAF15 are soluble nuclear RNA/DNA binding proteins that regulate mRNA splicing and/or stability and contain prion-like unstructured domains and nuclear/cytoplasmic trafficking signals. In neurons of patients with ALS/FTD these proteins have been found in cytoplasmic aggregates instead of their normal nuclear location. This suggests that impaired nucleocytoplasmic transport may be a general mechanism for neurotoxicity [3,66-71]. Indeed, impairing nuclear import of TDP-43 enhances neurotoxicity [72].

bioRxiv preprint doi: https://doi.org/10.1101/415927; this version posted September 13, 2018. The copyright holder for this preprint (which was not certified by peer review) is the author/funder. All rights reserved. No reuse allowed without permission.

While TDP-43, FUS and TAF-15 are found throughout the nucleus, CREST is found in nuclear bodies [73,74]. While TDP-43, and FUS quickly form cytoplasmic aggregates in yeast with little or no nuclear localization [29,30,35,53,75-77] we found here that CREST appeared in nuclear bodies with only occasional cytoplasmic foci. RNA has been found to help keep RNA binding proteins with prion-like domains soluble[78]. This is consistent with finding that FUS and TDP-43 are soluble in the nucleus but form aggregates in the cytoplasm. While the ALS associated proteins TDP-43, FUS and SOD1 form aggregates in patients, model systems and *in vitro*, these aggregates are sometime but not always classical amyloids. In yeast, FUS, but not TDP-43, aggregates stain with the amyloid dye thioflavin T [59]. Although both nuclear and cytoplasmic CREST foci appear to stain with thioflavin T and therefore contain amyloid, it is still tempting to speculate, by analogy with FUS and TDP-43, that the CREST cytoplasmic foci are more toxic than nuclear CREST. It is unknown if similar aggregates form in patients associated with neuronal death.

We found that heat stress induced CREST to leave the nucleus and partially co-localize with RNP granules. Furthermore, as seen for classic stress granule proteins, CREST returned to the nucleus following the heat stress. Many proteins associated with neurodegenerative disease contain intrinsically disordered regions that are required for their appearance in RNP granules. Evidence has been accumulating that RNP granules are incubators for the formation of pathogenic protein aggregates associated with neurodegenerative disease. It has been proposed that localization of proteins such as TDP-43, FUS and C9OFR72-encoded dipeptide repeat GR50 in high concentration in stress granules likely in a gel form, promotes their conversion into pathogenic amyloid-like aggregates[78-82].

In support of this model, RNP-granule formation has been shown to be strongly associated with neurodegeneration. This was accomplished with the aid of ATXN2, an RNP-protein that is required for

bioRxiv preprint doi: https://doi.org/10.1101/415927; this version posted September 13, 2018. The copyright holder for this preprint (which was not certified by peer review) is the author/funder. All rights reserved. No reuse allowed without permission.

RNP-granule formation. Three ALS associated proteins, TDP-43, FUS and C9OFR71-endoded dipeptide repeat GR50, have been shown to co-localize with ATXN2 RNP granules[40,79] in yeast, human or Drosophila S2 cells. Also, either reducing the level of ATXN2 or deleting one of its intrinsically disordered regions both reduced RNP-granule formation and reduced neurodegeneration caused by TDP-43, C9ORF72 dipeptide or FUS [79,83-85]. These results help explain why expansions of the polyQ regions in ATXN2 that increase the stability, and thus likely the level of ATXN2, are associated with neurodegenerative disease (susceptibility to ALS and type 2 spinocerebellar ataxia).

Here, using a yeast model system we report similar effects of PBP1, the yeast ATXN2 homolog, on CREST: overexpression of PBP1 causes CREST to co-localize with PBP1 in cytoplasmic granules; deletion of *PBP1* reduces toxicity of CREST. Overexpression of PBP1 has previously been shown to induce the formation of cytoplasmic PBP1 foci that[86] recruit TORC1 thereby down regulating TORC1 function[87]. PBP1 foci may similarly attract CREST to cytoplasmic granules which may promote CREST's conversion to a more toxic form. Surprisingly, overexpression of PBP1 prevented most CREST foci from staining with Thioflavin T. Possibly PBP1 reduces the amyloid nature of CREST foci or more likely the addition of PBP1 to CREST foci protects the CREST amyloid from the dye.

In mammals, endogenous CREST is a member of a chromatin remodeling complex and thereby activates transcription. When expressed in yeast we found that CREST releases telomeric silencing and causes flocculation. Thus we propose that even in yeast the heterologous CREST protein remodels chromatin causing transcriptional activation of telomerically located genes including those that cause flocculation (e.g. *FLO1, FLO5, FLO9* and *FLO10*). Likewise, a yeast chromatin remodeling complex protein, SWI1, is required for the expression of telomerically located *FLO* genes[88]. Interestingly, when SWI1 forms prion aggregates, flocculation is inhibited, presumably because the aggregated SWI1 is no longer able to function as a transcriptional activator[88]. We propose that *pbp1Δ* rescues CREST from its

bioRxiv preprint doi: https://doi.org/10.1101/415927; this version posted September 13, 2018. The copyright holder for this preprint (which was not certified by peer review) is the author/funder. All rights reserved. No reuse allowed without permission.

toxicity by reducing the level of toxic CREST aggregates formed and simultaneously enhancing the level of soluble CREST that is able to function to activate the *FLO* genes.

Our results extend the spectrum of ALS associated proteins that are affected by ATXN2 to include CREST. This supports the hypothesis that therapies that target ATXN2 may be effective for a wide range of neurodegenerative diseases.

Methods

Yeast strains and plasmids

Yeast strains and plasmids used are listed in Tables 1 and 2. Unless otherwise stated, yeast strain BY4741 (*MAT**a** his3Δ1 leu2Δ0 met15Δ0 ura3Δ0)* was used. Yeast transformation was by the lithium acetate method [89]. L3491 bearing an integrated copy of *ADH1-HTB1-mCh* was used to check CREST nuclear localization[35]. Unless otherwise stated, all overexpression plasmids were driven by the *GAL1* promoter. Gateway technology[90] was used to make CREST entry clone p2370 with BP reactions between pDONR221 (Invitrogen, Cat# 12536017) and a CREST fragment amplified from p2342 with PCR. The CREST fragment in p2370 was further transferred to p2380, p1764, p2387 and p2425 to respectively build p2381 (2μ *GAL1-CREST-EGFP*), p2375 (*CEN GAL1-CREST-EGFP*), p2389 (2μ *Gal-CREST-DsRED*) and p2391 (YIp *GAL-CREST-EGFP*) with LR reactions. To increase expression of *GAL1* controlled CREST, p798, containing human estrogen receptor hormone-binding domain fused to the *GAL4* DNA binding domain and the VP16 viral transcriptional activator (hER) was used.

Cultivation procedures

Standard media and growth conditions were used [91,92]. All liquid-culture experiments were carried out with mid-log-phase cells. Complex (YPD) yeast media contained 2% dextrose. Synthetic medium lacked

bioRxiv preprint doi: https://doi.org/10.1101/415927; this version posted September 13, 2018. The copyright holder for this preprint (which was not certified by peer review) is the author/funder. All rights reserved. No reuse allowed without permission.

a specific component, e.g. leucine, and contained 2% dextrose, e.g., SD-Leu (-Leu medium) or 2% galactose without (SGal-Leu) or with raffinose 2% (SRGal-Leu). Cells co-transformed with p798, containing hER, were grown in β-estradiol (1 μM) in glucose media to turn on expression of *GAL1* controlled CREST [52]. FOA medium containing 12 mg/l 5-fluoro-orotic acid and 12 mg/l uracil was used to score for telomeric silencing [93]. To prevent the accumulation of suppressor mutants that reverse CREST toxicity, pGAL1-CREST transformants were maintained on plasmid selective SD medium where CREST was not expressed. Patches were then replica-plated onto synthetic glycerol (2%) to identify petites that were dropped from further study. To analyze growth, non-petite transformants from SD plates were normalized in water to an OD_{600} of 2, serially diluted 10X. Finally about 5µl of diluted cell suspensions were spotted on plasmid selective SD, SGal or SD + β-estradiol using an MC48 (Dan-kar Corp, MA) spotter.

Scoring telomeric silencing

Telomeric silencing of the telomere-located *URA3* gene in strain GF513 was scored on the basis of growth of on -Ura and +FOA plates as described in the text [58]. Cells grown in plasmid selective SD medium overnight were harvested, washed, resuspended in water to OD_{600} of 2, spotted on FOA and –Ura media and incubated at 30°C for 3 days.

Western blot analysis

CREST was detected in precleared lysates separated by SDS-Page and blotted as described previously[94]. Blots were developed with GFP mouse antibody from Roche Applied Science (Indianapolis, IN) and PGK antibody from life technologies (Frederick, MD).

Visualization of aggregates and co-localization studies

Fluorescently labeled protein aggregates, were visualized in cells with a Nikon Eclipse E600 fluorescent microscope (100X oil immersion) equipped with FITC, YFP and mCh (respectively, chroma 49011, 49003

bioRxiv preprint doi: https://doi.org/10.1101/415927; this version posted September 13, 2018. The copyright holder for this preprint (which was not certified by peer review) is the author/funder. All rights reserved. No reuse allowed without permission.

and 49008) filter cubes. To visualize nuclei, cells with the integrated HTB1-mCh nuclear marker were used[35].

Flocculation Assay

Flocculation was assayed by resuspending 2 d cultures in 50 mM EDTA in water. Since flocculation requires the presence of Ca^{2+} ions[95], this removed clumping so cells could be accurately normalized to OD_{600} of 10. $CaCl_2$ was then added to 100mM to chelate the EDTA and restore flocculence. Cells were photographed after they were allowed to settle for 15 min. The level of precipitation of cells is a measure of the flocculence.

Thioflavin T Staining

Yeast cells were stained with Thioflavin T according to a protocol adapted from [29] with the addition of two extra washes in PMST [0.1M KPO_4 (pH 7.5), 1 mM $MgCl_2$, 1 M Sorbitol, 0.1% Tween 20].

Data Availability

No datasets were generated during the current study. The datasets analyzed during the current study are publically available at https://www.yeastgenome.org/.

bioRxiv preprint doi: https://doi.org/10.1101/415927; this version posted September 13, 2018. The copyright holder for this preprint (which was not certified by peer review) is the author/funder. All rights reserved. No reuse allowed without permission.

REFERENCES

1 Bertram, L. & Tanzi, R. E. The genetic epidemiology of neurodegenerative disease. *The Journal of clinical investigation* **115**, 1449-1457, doi:10.1172/JCI24761 (2005).

2 Chen, S., Sayana, P., Zhang, X. & Le, W. Genetics of amyotrophic lateral sclerosis: an update. *Molecular neurodegeneration* **8**, 28, doi:10.1186/1750-1326-8-28 (2013).

3 Barmada, S. J. *et al.* Cytoplasmic mislocalization of TDP-43 is toxic to neurons and enhanced by a mutation associated with familial amyotrophic lateral sclerosis. *The Journal of neuroscience : the official journal of the Society for Neuroscience* **30**, 639-649, doi:10.1523/JNEUROSCI.4988-09.2010 (2010).

4 Liebman, S. W. & Chernoff, Y. O. Prions in yeast. *Genetics* **191**, 1041-1072, doi:10.1534/genetics.111.137760 (2012).

5 Wickner, R. B. [URE3] as an altered URE2 protein: evidence for a prion analog in Saccharomyces cerevisiae. *Science* **264**, 566-569 (1994).

6 Wickner, R. B., Masison, D. C. & Edskes, H. K. [PSI] and [URE3] as yeast prions. *Yeast* **11**, 1671-1685, doi:10.1002/yea.320111609 (1995).

7 Sondheimer, N. & Lindquist, S. Rnq1: an epigenetic modifier of protein function in yeast. *Molecular cell* **5**, 163-172 (2000).

8 Derkatch, I. L., Bradley, M. E., Hong, J. Y. & Liebman, S. W. Prions affect the appearance of other prions: the story of [PIN(+)]. *Cell* **106**, 171-182 (2001).

9 Patel, B. K., Gavin-Smyth, J. & Liebman, S. W. The yeast global transcriptional co-repressor protein Cyc8 can propagate as a prion. *Nat Cell Biol* **11**, 344-349, doi:10.1038/ncb1843 (2009).

10 Suzuki, G., Shimazu, N. & Tanaka, M. A yeast prion, Mod5, promotes acquired drug resistance and cell survival under environmental stress. *Science* **336**, 355-359, doi:10.1126/science.1219491 (2012).

bioRxiv preprint doi: https://doi.org/10.1101/415927; this version posted September 13, 2018. The copyright holder for this preprint (which was not certified by peer review) is the author/funder. All rights reserved. No reuse allowed without permission.

11 Patino, M. M., Liu, J. J., Glover, J. R. & Lindquist, S. Support for the prion hypothesis for inheritance of a phenotypic trait in yeast. *Science* **273**, 622-626 (1996).

12 Du, Z., Park, K. W., Yu, H., Fan, Q. & Li, L. Newly identified prion linked to the chromatin-remodeling factor Swi1 in Saccharomyces cerevisiae. *Nature genetics* **40**, 460-465, doi:10.1038/ng.112 (2008).

13 Paushkin, S. V., Kushnirov, V. V., Smirnov, V. N. & Ter-Avanesyan, M. D. Propagation of the yeast prion-like [psi+] determinant is mediated by oligomerization of the SUP35-encoded polypeptide chain release factor. *The EMBO journal* **15**, 3127-3134 (1996).

14 Nizhnikov, A. A. *et al.* Proteomic screening for amyloid proteins. *PloS one* **9**, e116003, doi:10.1371/journal.pone.0116003 (2014).

15 Pezza, J. A., Villali, J., Sindi, S. S. & Serio, T. R. Amyloid-associated activity contributes to the severity and toxicity of a prion phenotype. *Nature communications* **5**, 4384, doi:10.1038/ncomms5384 (2014).

16 Du, Z. & Li, L. Investigating the interactions of yeast prions: [SWI+], [PSI+], and [PIN+]. *Genetics* **197**, 685-700, doi:10.1534/genetics.114.163402 (2014).

17 Derkatch, I. L., Bradley, M. E., Zhou, P., Chernoff, Y. O. & Liebman, S. W. Genetic and environmental factors affecting the de novo appearance of the [PSI+] prion in Saccharomyces cerevisiae. *Genetics* **147**, 507-519 (1997).

18 Derkatch, I. L. *et al.* Effects of Q/N-rich, polyQ, and non-polyQ amyloids on the de novo formation of the [PSI+] prion in yeast and aggregation of Sup35 in vitro. *Proceedings of the National Academy of Sciences of the United States of America* **101**, 12934-12939, doi:10.1073/pnas.0404968101 (2004).

19 Liebman, S. W., Bagriantsev, S. N. & Derkatch, I. L. Biochemical and genetic methods for characterization of [PIN+] prions in yeast. *Methods* **39**, 23-34, doi:10.1016/j.ymeth.2006.04.010 (2006).

bioRxiv preprint doi: https://doi.org/10.1101/415927; this version posted September 13, 2018. The copyright holder for this preprint (which was not certified by peer review) is the author/funder. All rights reserved. No reuse allowed without permission.

20 Derkatch, I. L. & Liebman, S. W. Prion-prion interactions. *Prion* **1**, 161-169 (2007).

21 Sharma, J. & Liebman, S. W. Exploring the basis of [PIN(+)] variant differences in [PSI(+)] induction. *J Mol Biol* **425**, 3046-3059, doi:10.1016/j.jmb.2013.06.006 (2013).

22 Sharma, J. & Liebman, S. W. Variant-specific prion interactions: Complicating factors. *Cellular logistics* **3**, e25698, doi:10.4161/cl.25698 (2013).

23 Vitrenko, Y. A., Gracheva, E. O., Richmond, J. E. & Liebman, S. W. Visualization of aggregation of the Rnq1 prion domain and cross-seeding interactions with Sup35NM. *The Journal of biological chemistry* **282**, 1779-1787, doi:10.1074/jbc.M609269200 (2007).

24 Yang, Z., Hong, J. Y., Derkatch, I. L. & Liebman, S. W. Heterologous gln/asn-rich proteins impede the propagation of yeast prions by altering chaperone availability. *PLoS genetics* **9**, e1003236, doi:10.1371/journal.pgen.1003236 (2013).

25 Serio, T. R. [PIN+]ing down the mechanism of prion appearance. *FEMS yeast research* **18**, doi:10.1093/femsyr/foy026 (2018).

26 Meriin, A. B. *et al.* Huntington toxicity in yeast model depends on polyglutamine aggregation mediated by a prion-like protein Rnq1. *The Journal of cell biology* **157**, 997-1004, doi:10.1083/jcb.200112104 (2002).

27 Gokhale, K. C., Newnam, G. P., Sherman, M. Y. & Chernoff, Y. O. Modulation of prion-dependent polyglutamine aggregation and toxicity by chaperone proteins in the yeast model. *The Journal of biological chemistry* **280**, 22809-22818, doi:10.1074/jbc.M500390200 (2005).

28 Holmes, D. L., Lancaster, A. K., Lindquist, S. & Halfmann, R. Heritable remodeling of yeast multicellularity by an environmentally responsive prion. *Cell* **153**, 153-165, doi:10.1016/j.cell.2013.02.026 (2013).

29 Johnson, B. S., McCaffery, J. M., Lindquist, S. & Gitler, A. D. A yeast TDP-43 proteinopathy model: Exploring the molecular determinants of TDP-43 aggregation and cellular toxicity.

bioRxiv preprint doi: https://doi.org/10.1101/415927; this version posted September 13, 2018. The copyright holder for this preprint (which was not certified by peer review) is the author/funder. All rights reserved. No reuse allowed without permission.

Proceedings of the National Academy of Sciences of the United States of America **105**, 6439-6444, doi:10.1073/pnas.0802082105 (2008).

30 Ju, S. *et al.* A yeast model of FUS/TLS-dependent cytotoxicity. *PLoS Biol* **9**, e1001052, doi:10.1371/journal.pbio.1001052 (2011).

31 Kryndushkin, D., Ihrke, G., Piermartiri, T. C. & Shewmaker, F. A yeast model of optineurin proteinopathy reveals a unique aggregation pattern associated with cellular toxicity. *Molecular microbiology* **86**, 1531-1547, doi:10.1111/mmi.12075 (2012).

32 Kryndushkin, D. & Shewmaker, F. Modeling ALS and FTLD proteinopathies in yeast: an efficient approach for studying protein aggregation and toxicity. *Prion* **5**, 250-257, doi:10.4161/pri.17229 (2011).

33 Di Gregorio, S. E. & Duennwald, M. L. Yeast as a model to study protein misfolding in aged cells. *FEMS yeast research* **18**, doi:10.1093/femsyr/foy054 (2018).

34 Kurahashi, H., Ishiwata, M., Shibata, S. & Nakamura, Y. A regulatory role of the Rnq1 nonprion domain for prion propagation and polyglutamine aggregates. *Molecular and cellular biology* **28**, 3313-3323, doi:10.1128/MCB.01900-07 (2008).

35 Park, S. K. *et al.* Overexpression of the essential Sis1 chaperone reduces TDP-43 effects on toxicity and proteolysis. *PLoS genetics* **13**, e1006805, doi:10.1371/journal.pgen.1006805 (2017).

36 Treusch, S. *et al.* Functional links between Abeta toxicity, endocytic trafficking, and Alzheimer's disease risk factors in yeast. *Science* **334**, 1241-1245, doi:10.1126/science.1213210 (2011).

37 Park, S. K., Ratia, K., Ba, M., Valencik, M. & Liebman, S. W. Inhibition of Abeta42 oligomerization in yeast by a PICALM ortholog and certain FDA approved drugs. *Microb Cell* **3**, 53-64, doi:10.15698/mic2016.02.476 (2016).

38 Rosenthal, S. L. *et al.* Beta-amyloid toxicity modifier genes and the risk of Alzheimer's disease. *American journal of neurodegenerative disease* **1**, 191-198 (2012).

bioRxiv preprint doi: https://doi.org/10.1101/415927; this version posted September 13, 2018. The copyright holder for this preprint (which was not certified by peer review) is the author/funder. All rights reserved. No reuse allowed without permission.

39 Gitler, A. D. *et al.* Alpha-synuclein is part of a diverse and highly conserved interaction network that includes PARK9 and manganese toxicity. *Nature genetics* **41**, 308-315, doi:10.1038/ng.300 (2009).

40 Elden, A. C. *et al.* Ataxin-2 intermediate-length polyglutamine expansions are associated with increased risk for ALS. *Nature* **466**, 1069-1075, doi:10.1038/nature09320 (2010).

41 Auburger, G., Sen, N. E., Meierhofer, D., Basak, A. N. & Gitler, A. D. Efficient Prevention of Neurodegenerative Diseases by Depletion of Starvation Response Factor Ataxin-2. *Trends in neurosciences* **40**, 507-516, doi:10.1016/j.tins.2017.06.004 (2017).

42 Figley, M. D., Thomas, A. & Gitler, A. D. Evaluating noncoding nucleotide repeat expansions in amyotrophic lateral sclerosis. *Neurobiology of aging* **35**, 936 e931-934, doi:10.1016/j.neurobiolaging.2013.09.024 (2014).

43 Gispert, S. *et al.* The modulation of Amyotrophic Lateral Sclerosis risk by ataxin-2 intermediate polyglutamine expansions is a specific effect. *Neurobiology of disease* **45**, 356-361, doi:10.1016/j.nbd.2011.08.021 (2012).

44 Yu, Z. *et al.* PolyQ repeat expansions in ATXN2 associated with ALS are CAA interrupted repeats. *PloS one* **6**, e17951, doi:10.1371/journal.pone.0017951 (2011).

45 Teyssou, E. *et al.* Genetic analysis of SS18L1 in French amyotrophic lateral sclerosis. *Neurobiology of aging* **35**, doi:ARTN 1213.e9 10.1016/j.neurobiolaging.2013.11.023 (2014).

46 Chesi, A. *et al.* Exome sequencing to identify de novo mutations in sporadic ALS trios. *Nature neuroscience* **16**, 851-855, doi:10.1038/nn.3412 (2013).

47 Middeljans, E. *et al.* SS18 together with animal-specific factors defines human BAF-type SWI/SNF complexes. *PloS one* **7**, e33834, doi:10.1371/journal.pone.0033834 (2012).

48 Hodges, C., Kirkland, J. G. & Crabtree, G. R. The Many Roles of BAF (mSWI/SNF) and PBAF Complexes in Cancer. *Cold Spring Harbor perspectives in medicine* **6**, doi:10.1101/cshperspect.a026930 (2016).

bioRxiv preprint doi: https://doi.org/10.1101/415927; this version posted September 13, 2018. The copyright holder for this preprint (which was not certified by peer review) is the author/funder. All rights reserved. No reuse allowed without permission.

49 Staahl, B. T. *et al.* Kinetic analysis of npBAF to nBAF switching reveals exchange of SS18 with CREST and integration with neural developmental pathways. *The Journal of neuroscience : the official journal of the Society for Neuroscience* **33**, 10348-10361, doi:10.1523/JNEUROSCI.1258-13.2013 (2013).

50 Kukharsky, M. S. *et al.* Calcium-responsive transactivator (CREST) protein shares a set of structural and functional traits with other proteins associated with amyotrophic lateral sclerosis. *Molecular neurodegeneration* **10**, 20, doi:10.1186/s13024-015-0014-y (2015).

51 Pradhan, A. & Liu, Y. A multifunctional domain of the calcium-responsive transactivator (CREST) that inhibits dendritic growth in cultured neurons. *The Journal of biological chemistry* **280**, 24738-24743, doi:10.1074/jbc.M504018200 (2005).

52 Derkatch, I. L., Chernoff, Y. O., Kushnirov, V. V., Inge-Vechtomov, S. G. & Liebman, S. W. Genesis and variability of [PSI] prion factors in Saccharomyces cerevisiae. *Genetics* **144**, 1375-1386 (1996).

53 Park, S. K. *et al.* Overexpression of a conserved HSP40 chaperone reduces toxicity of several neurodegenerative disease proteins. *Prion* **12**, 16-22, doi:10.1080/19336896.2017.1423185 (2018).

54 Mueller, J. E., Canze, M. & Bryk, M. The requirements for COMPASS and Paf1 in transcriptional silencing and methylation of histone H3 in Saccharomyces cerevisiae. *Genetics* **173**, 557-567, doi:10.1534/genetics.106.055400 (2006).

55 Guo, B., Styles, C. A., Feng, Q. & Fink, G. R. A Saccharomyces gene family involved in invasive growth, cell-cell adhesion, and mating. *Proceedings of the National Academy of Sciences of the United States of America* **97**, 12158-12163, doi:10.1073/pnas.220420397 (2000).

56 Dietvorst, J. & Brandt, A. Flocculation in Saccharomyces cerevisiae is repressed by the COMPASS methylation complex during high-gravity fermentation. *Yeast* **25**, 891-901, doi:10.1002/yea.1643 (2008).

bioRxiv preprint doi: https://doi.org/10.1101/415927; this version posted September 13, 2018. The copyright holder for this preprint (which was not certified by peer review) is the author/funder. All rights reserved. No reuse allowed without permission.

57 Gottschling, D. E., Aparicio, O. M., Billington, B. L. & Zakian, V. A. Position effect at S. cerevisiae telomeres: reversible repression of Pol II transcription. *Cell* **63**, 751-762 (1990).

58 Huang, H., Kahana, A., Gottschling, D. E., Prakash, L. & Liebman, S. W. The ubiquitin-conjugating enzyme Rad6 (Ubc2) is required for silencing in Saccharomyces cerevisiae. *Molecular and cellular biology* **17**, 6693-6699 (1997).

59 Fushimi, K. *et al.* Expression of human FUS/TLS in yeast leads to protein aggregation and cytotoxicity, recapitulating key features of FUS proteinopathy. *Protein Cell* **2**, 141-149, doi:10.1007/s13238-011-1014-5 (2011).

60 Zhou, P., Derkatch, I. L. & Liebman, S. W. The relationship between visible intracellular aggregates that appear after overexpression of Sup35 and the yeast prion-like elements [PSI(+)] and [PIN(+)]. *Molecular microbiology* **39**, 37-46 (2001).

61 Derkatch, I. L. *et al.* Dependence and independence of [PSI(+)] and [PIN(+)]: a two-prion system in yeast? *The EMBO journal* **19**, 1942-1952, doi:10.1093/emboj/19.9.1942 (2000).

62 Fuentealba, R. A. *et al.* Interaction with polyglutamine aggregates reveals a Q/N-rich domain in TDP-43. *The Journal of biological chemistry* **285**, 26304-26314, doi:10.1074/jbc.M110.125039 (2010).

63 Doi, H. *et al.* RNA-binding protein TLS is a major nuclear aggregate-interacting protein in huntingtin exon 1 with expanded polyglutamine-expressing cells. *The Journal of biological chemistry* **283**, 6489-6500, doi:10.1074/jbc.M705306200 (2008).

64 Seidel, G. *et al.* Quantitative Global Proteomics of Yeast PBP1 Deletion Mutants and Their Stress Responses Identifies Glucose Metabolism, Mitochondrial, and Stress Granule Changes. *Journal of proteome research* **16**, 504-515, doi:10.1021/acs.jproteome.6b00647 (2017).

65 Olbertz, J. H. The protein SS18L1 is a potent suppressor of polyQ mediated huntingtin aggregation and toxicity. *Dissertation* **Adviser Dr. Erich Wanker** (2012).

bioRxiv preprint doi: https://doi.org/10.1101/415927; this version posted September 13, 2018. The copyright holder for this preprint (which was not certified by peer review) is the author/funder. All rights reserved. No reuse allowed without permission.

66 Kapeli, K. *et al.* Distinct and shared functions of ALS-associated proteins TDP-43, FUS and TAF15 revealed by multisystem analyses. *Nature communications* **7**, 12143, doi:10.1038/ncomms12143 (2016).

67 Couthouis, J. *et al.* A yeast functional screen predicts new candidate ALS disease genes. *Proceedings of the National Academy of Sciences of the United States of America* **108**, 20881-20890, doi:10.1073/pnas.1109434108 (2011).

68 Neumann, M. *et al.* Ubiquitinated TDP-43 in frontotemporal lobar degeneration and amyotrophic lateral sclerosis. *Science* **314**, 130-133, doi:10.1126/science.1134108 (2006).

69 Kwiatkowski, T. J., Jr. *et al.* Mutations in the FUS/TLS gene on chromosome 16 cause familial amyotrophic lateral sclerosis. *Science* **323**, 1205-1208, doi:10.1126/science.1166066 (2009).

70 Vance, C. *et al.* Mutations in FUS, an RNA processing protein, cause familial amyotrophic lateral sclerosis type 6. *Science* **323**, 1208-1211, doi:10.1126/science.1165942 (2009).

71 Jovicic, A., Paul, J. W., 3rd & Gitler, A. D. Nuclear transport dysfunction: a common theme in amyotrophic lateral sclerosis and frontotemporal dementia. *Journal of neurochemistry* **138 Suppl 1**, 134-144, doi:10.1111/jnc.13642 (2016).

72 Archbold, H. C. *et al.* TDP43 nuclear export and neurodegeneration in models of amyotrophic lateral sclerosis and frontotemporal dementia. *Scientific reports* **8**, 4606, doi:10.1038/s41598-018-22858-w (2018).

73 Naganuma, T. *et al.* Alternative 3'-end processing of long noncoding RNA initiates construction of nuclear paraspeckles. *The EMBO journal* **31**, 4020-4034, doi:10.1038/emboj.2012.251 (2012).

74 Pradhan, A. & Liu, Y. The calcium-responsive transactivator recruits CREB binding protein to nuclear bodies. *Neuroscience letters* **370**, 191-195, doi:10.1016/j.neulet.2004.08.062 (2004).

bioRxiv preprint doi: https://doi.org/10.1101/415927; this version posted September 13, 2018. The copyright holder for this preprint (which was not certified by peer review) is the author/funder. All rights reserved. No reuse allowed without permission.

75 Kryndushkin, D., Wickner, R. B. & Shewmaker, F. FUS/TLS forms cytoplasmic aggregates, inhibits cell growth and interacts with TDP-43 in a yeast model of amyotrophic lateral sclerosis. *Protein Cell* **2**, 223-236, doi:10.1007/s13238-011-1525-0 (2011).

76 Armakola, M. *et al.* Inhibition of RNA lariat debranching enzyme suppresses TDP-43 toxicity in ALS disease models. *Nature genetics* **44**, 1302-1309, doi:10.1038/ng.2434 (2012).

77 Sun, Z. *et al.* Molecular determinants and genetic modifiers of aggregation and toxicity for the ALS disease protein FUS/TLS. *PLoS Biol* **9**, e1000614, doi:10.1371/journal.pbio.1000614 (2011).

78 Maharana, S. *et al.* RNA buffers the phase separation behavior of prion-like RNA binding proteins. *Science* **360**, 918-921, doi:10.1126/science.aar7366 (2018).

79 Bakthavachalu, B. *et al.* RNP-Granule Assembly via Ataxin-2 Disordered Domains Is Required for Long-Term Memory and Neurodegeneration. *Neuron* **98**, 754-766 e754, doi:10.1016/j.neuron.2018.04.032 (2018).

80 Li, Y. R., King, O. D., Shorter, J. & Gitler, A. D. Stress granules as crucibles of ALS pathogenesis. *The Journal of cell biology* **201**, 361-372, doi:10.1083/jcb.201302044 (2013).

81 Li, S. *et al.* Genetic interaction of hnRNPA2B1 and DNAJB6 in a Drosophila model of multisystem proteinopathy. *Human molecular genetics* **25**, 936-950, doi:10.1093/hmg/ddv627 (2016).

82 Monahan, Z., Shewmaker, F. & Pandey, U. B. Stress granules at the intersection of autophagy and ALS. *Brain research* **1649**, 189-200, doi:10.1016/j.brainres.2016.05.022 (2016).

83 Becker, L. A. *et al.* Therapeutic reduction of ataxin-2 extends lifespan and reduces pathology in TDP-43 mice. *Nature* **544**, 367-371, doi:10.1038/nature22038 (2017).

84 Lee, K. H. *et al.* C9orf72 Dipeptide Repeats Impair the Assembly, Dynamics, and Function of Membrane-Less Organelles. *Cell* **167**, 774-788 e717, doi:10.1016/j.cell.2016.10.002 (2016).

85 Scoles, D. R. *et al.* Antisense oligonucleotide therapy for spinocerebellar ataxia type 2. *Nature* **544**, 362-366, doi:10.1038/nature22044 (2017).

bioRxiv preprint doi: https://doi.org/10.1101/415927; this version posted September 13, 2018. The copyright holder for this preprint (which was not certified by peer review) is the author/funder. All rights reserved. No reuse allowed without permission.

86 Swisher, K. D. & Parker, R. Localization to, and effects of Pbp1, Pbp4, Lsm12, Dhh1, and Pab1 on stress granules in Saccharomyces cerevisiae. *PloS one* **5**, e10006, doi:10.1371/journal.pone.0010006 (2010).

87 Takahara, T. & Maeda, T. Transient sequestration of TORC1 into stress granules during heat stress. *Molecular cell* **47**, 242-252, doi:10.1016/j.molcel.2012.05.019 (2012).

88 Goncharoff, D. K., Du, Z. & Li, L. A brief overview of the Swi1 prion-[SWI+]. *FEMS yeast research* **18**, doi:10.1093/femsyr/foy061 (2018).

89 Gietz, R. D. & Schiestl, R. H. High-efficiency yeast transformation using the LiAc/SS carrier DNA/PEG method. *Nature protocols* **2**, 31-34, doi:10.1038/nprot.2007.13 (2007).

90 Alberti, S., Gitler, A. D. & Lindquist, S. A suite of Gateway cloning vectors for high-throughput genetic analysis in Saccharomyces cerevisiae. *Yeast* **24**, 913-919, doi:10.1002/yea.1502 (2007).

91 Sherman F, F. G., Hicks JB. *Methods in Yeast Genetics*. (Cold Spring Harbor Press, 1986).

92 Sikorski, R. S. & Hieter, P. A system of shuttle vectors and yeast host strains designed for efficient manipulation of DNA in Saccharomyces cerevisiae. *Genetics* **122**, 19-27 (1989).

93 Boeke, J. D., LaCroute, F. & Fink, G. R. A positive selection for mutants lacking orotidine-5'-phosphate decarboxylase activity in yeast: 5-fluoro-orotic acid resistance. *Molecular & general genetics : MGG* **197**, 345-346 (1984).

94 Bagriantsev, S. N., Gracheva, E. O., Richmond, J. E. & Liebman, S. W. Variant-specific [PSI+] infection is transmitted by Sup35 polymers within [PSI+] aggregates with heterogeneous protein composition. *Molecular biology of the cell* **19**, 2433-2443, doi:10.1091/mbc.E08-01-0078 (2008).

95 Stratford, M. Yeast flocculation:Calcium specificity. *Yeast* **5**, 487-496 (1989).

96 Brachmann, C. B. *et al.* Designer deletion strains derived from Saccharomyces cerevisiae S288C: a useful set of strains and plasmids for PCR-mediated gene disruption and other applications.

bioRxiv preprint doi: https://doi.org/10.1101/415927; this version posted September 13, 2018. The copyright holder for this preprint (which was not certified by peer review) is the author/funder. All rights reserved. No reuse allowed without permission.

Yeast **14**, 115-132, doi:10.1002/(SICI)1097-0061(19980130)14:2<115::AID-YEA204>3.0.CO;2-2 (1998).

97 Winzeler, E. A. *et al.* Functional characterization of the S. cerevisiae genome by gene deletion and parallel analysis. *Science* **285**, 901-906 (1999).

98 Louvion, J. F., Havaux-Copf, B. & Picard, D. Fusion of GAL4-VP16 to a steroid-binding domain provides a tool for gratuitous induction of galactose-responsive genes in yeast. *Gene* **131**, 129-134 (1993).

99 Buchan, J. R., Muhlrad, D. & Parker, R. P bodies promote stress granule assembly in Saccharomyces cerevisiae. *The Journal of cell biology* **183**, 441-455, doi:10.1083/jcb.200807043 (2008).

bioRxiv preprint doi: https://doi.org/10.1101/415927; this version posted September 13, 2018. The copyright holder for this preprint (which was not certified by peer review) is the author/funder. All rights reserved. No reuse allowed without permission.

Acknowledgements

We thank Tatyana Shelkovnika, Cardiff U., UK for plasmids and helpful comments on the manuscript. We also thank Ross Buchan, U. of Arizona; Bernd Bukau, U. Heidelberg; the late Susan Lindquist, MIT and Aaron Gitler, Stanford U., for plasmids. In addition we thank William Eom for helpful comments on the manuscript. This work was supported National Institutes of Health Grant R01GM056350 (SWL).

Author Contributions

SP did all the experiments. SP, SKP and SWL designed experiments. SWL wrote the body of the paper with help from SP and SKP. SP wrote the Methods and Figure legends with help from SKP and SWL.

Competing Interests

The authors declare no competing interests.

bioRxiv preprint doi: https://doi.org/10.1101/415927; this version posted September 13, 2018. The copyright holder for this preprint (which was not certified by peer review) is the author/funder. All rights reserved. No reuse allowed without permission.

Figure Legends:

Figure 1. Expression of human CREST in yeast is toxic. Shown is the growth of cells carrying vectors encoding *GAL-CREST-GFP* and a fusion protein that promotes induction of the *GAL* promoter in the presence of estradiol (pβ-est) spotted on plasmid selective glucose plates without estradiol where CREST-GFP expression is uninduced (No β-Estradiol), or with 1 μM β-estradiol where CREST-GFP expression is induced (+β-Estradiol). Duplicates are independent transformants or integrants. Cells grown on plasmid selective glucose plates were diluted to OD_{600} =2 and then serially diluted 10-fold and spotted on the plates shown. (**a)** *CREST-GFP expressed from a CEN plasmid inhibits growth.* CREST-GFP CEN vector (p2375) and control GFP vector (v, p1764) were used. (**b**) *CREST-GFP expressed from a 2μ plasmid inhibits growth.* CREST-GFP 2μ vector (p2381) and the GFP vector (v, p2380) were used. (**c**) *Integrated CREST-GFP is toxic.* CREST-GFP was expressed in strain L3536 with integrated p2391 and the control GFP vector (v) was p2380. Strain 74D-694 [*PIN*$^+$] was used for the *CEN* and integrated vector experiments (**a** and **c**) while strain BY4741 [*PIN*$^+$] was used for the 2μ vector experiments (b). The pβ-est plasmid expressing the fusion activator that is responsive to β-estradiol is p798, and p2186 was used as its control (v). (**d**) *The [PIN$^+$] prion enhances toxicity of CREST in yeast.* Shown is the growth of [*PIN*$^+$] and [*pin*$^-$] BY4741 cells carrying 2μ vectors encoding *GAL-CREST-GFP* (p2381) and the pβ-est plasmid (p798) that promotes induction of the *GAL* promoter in the presence of estradiol (or empty control p2186, v) spotted on plasmid selective glucose plates without estradiol where CREST-GFP expression is uninduced (No β-Estradiol), or with 1 μM β-estradiol where CREST-GFP expression is induced (+β-Estradiol). Duplicates are independent transformants. Cells were adjusted to OD_{600} =2, serially diluted and spotted on the plates that were incubated for 3 days at 30°C.

Figure 2. Expression of CREST enhances yeast flocculation. (**a**) *CREST but not TDP-43 or FUS over expression enhances flocculation.* Transformants of BY4741 [*PIN*$^+$] containing *CEN GAL* vectors

bioRxiv preprint doi: https://doi.org/10.1101/415927; this version posted September 13, 2018. The copyright holder for this preprint (which was not certified by peer review) is the author/funder. All rights reserved. No reuse allowed without permission.

expressing FUS-YFP (p2043), TDP-43-YFP (p2042), CREST-GFP (p2375) or control vector (v, p1764) are shown. (**b**) *Deletion of PBP1 enhances flocculation.* Three different transformants of Gal1-CREST-GFP 2μ (CREST, p2381) and control vector (p2380) into *PBP1* (Wild-type) and *pbp1Δ* BY4741 [*PIN*$^+$] strains are shown. Flocculance was measured after transformants were grown in plasmid selective SRGal for 48 hrs. (**c**) *Expression of CREST reduces telomeric silencing.* Growth of UCC3537 (*MAT***a** *ura3-52 lys2-801 ade2-101 trp1-Δ63 his3-Δ200 leu2-Δ1 URA3-TEL-VII-L*) transformed with p*GAL-CREST-GFP* (p2381,↑CREST), or empty control vector (p2380, No CREST), grown on plasmid selective glucose plates, suspended in water to OD_{600}=2, serially diluted 10X and spotted (3μl) on plasmid selective SGal plates containing uracil (+ Ura), lacking uracil (-Ura) or containing 5-FOA (+FOA) is shown in left two columns. For a control, on the right, UCC3537 (*RAD6+*) and isogenic L1642 (*rad6::LEU2*) [58] were serially diluted and spotted on glucose +Ura, -Ura and +FOA plates.

Fig. 3. Human CREST expressed in yeast forms largely nuclear dots with occasional cytoplasmic foci. (**a**) *CREST-GFP expressed in yeast*. BY4741 [*PIN*$^+$] transformed with either the wild *GAL-CREST-GFP* 2μ vector (p2381) was induced for 6 or 24 hrs by growth in plasmid selective SRGal medium and examined under a fluorescent microscope. Shown is bright field plus fluorescence (left) and just fluorescence (right). (**b**) *Co-localization of wild-type CREST-GFP aggregates and nuclear marker HTB1-mCh*. Strain L3496 with integrated plasmid encoding ADH1-HTB1-mCh (pRS305-HTB1-mCh) transformed with *CEN GAL-CREST-GFP* (p2375) was grown on plasmid selective SRGal medium for 24 hrs and examined. (**c**) CREST aggregates stain with the amyloid dye thioflavin T (ThT), but overexpression of PBP1 inhibits this. L3491 containing HTB1-mCherry nuclear marker transformed with *GAL1-TDP-43-YFP* (p2042) as negative control, with *GAL-FUS-YFP* (p2043) as a positive control, *CREST-YFP* (p2471) or *CREST-YFP* plus *GAL-PBP1* (p2228) (↑PBP1 CREST YFP) were grown in plasmid selective SRGAL medium overnight. ThT

bioRxiv preprint doi: https://doi.org/10.1101/415927; this version posted September 13, 2018. The copyright holder for this preprint (which was not certified by peer review) is the author/funder. All rights reserved. No reuse allowed without permission.

fluorescence was detected with a CFP filter. CFP was recolored green and YFP recolored red to facilitate visualization of merged pictures. Cell boundaries are drawn.

Fig. 4 Overexpression of PBP1 enhances cytoplasmic aggregation of CREST and *pbp1Δ* reduces CREST toxicity. (**a**) *Overexpression of PBP1 enhances cytoplasmic aggregation of CREST*. BY4741 [*PIN*$^+$] or [*pin*$^-$] were co-transformed with plasmids expressing *GAL-CREST-GFP* (p2381) and either *CEN GAL-PBP1* (p2228) or an empty control vector (p2229). Nine transformants each with (↑PBP1) and without the *PBP1* plasmid (Control) were patched on plasmid selective glucose media, which was velveteen replica-plated to plasmid selective SGal medium the next day and examined with a fluorescent microscope after 24 hrs of incubation. All [*PIN*$^+$] or [*pin*$^-$] transformants with overexpressed PBP1 had a dramatic increase in cytoplasmic foci compared with transformants without overexpressed PBP1. Representative cells of each type are shown and cell membranes are outlined. (**b**) *Overexpression or deletion of PBP1 does not significantly change the level of CREST.* Left: Western blot of BY4741 (L3270) transformed with *GAL-CREST-GFP* (p2381) and either *CEN GAL-PBP1* (p2228) (↑PBP1) or an empty vector (p2229) (control) that were grown in liquid plasmid selective SRGal media for 36 hrs. Right: Western blot of isogenic BY4741 strains with (*pbp1Δ*), and with wild-type *PBP1* (Control), transformed with *GAL-CREST-GFP* (p2381)*.* Also shown (- CREST) is control with *GAL-GFP* (p2380) instead of CREST in *pbp1Δ* strain. Blots were probed with GFP antibody to detect CREST and then were stripped and reprobed with PGK antibody. PGK was used as a loading control. Full gels are shown in supplemental Fig. 1. (**c**) *CREST co-localizes with PBP1 in RNP granules induced by PBP1 overexpression. GAL-CREST-DsRED* (p2389) or control DsRED empty vector (p2387) and *GAL-PBP1-EGFP* (p2228) were co-transformed into BY4741 (L3270). Transformants patched on plasmid selective glucose medium were velveteen replica-plated to plasmid selective SGal and the examined with a fluorescent microscope after 24 hrs growth. (**d**) *Deletion of PBP1 reduces toxicity of CREST.* Independent transformants of BY4741 without (*PBP1*, L3270) and with the deletion (L3539, *pbp1Δ*) carrying *GAL-CREST-GFP* (p2381) or empty GFP control

bioRxiv preprint doi: https://doi.org/10.1101/415927; this version posted September 13, 2018. The copyright holder for this preprint (which was not certified by peer review) is the author/funder. All rights reserved. No reuse allowed without permission.

plasmid (p2380, v) and plasmid pβ-est (p798) expressing the fusion activator that is responsive to β-estradiol, were spotted and grown on plasmid selective media with (induced) and without (uninduced) β-estradiol. (**e**) *Overexpression of PBP1 is toxic.* Serial dilutions of transformants of BY4741 [*PIN*$^{+}$] with *pGAL1-CREST-GFP* (p2381), or pGFP control (p2380, v) and *pGAL1-PBP1* (p2228), or empty control (p2229, v) plasmids, were spotted on plasmid selective dextrose (non-inducing) and galactose (inducing) plates, which were photographed after 3 (dextrose) or 4 (galactose) days of incubation at 30˚C.

Fig. 5 CREST does not facilitate induction of [*PSI*$^{+}$]. Isogenic [*PIN*$^{+}$] (L1749) and [*pin*$^{-}$] (L2910) strains transformed with plasmids encoding *GAL-CREST-WT-DsRed* (p2389) and *CUP1-SUP35NM-GFP* (p1181) were patched on plasmid selective SGal plates with 50 μM CuSO4 and grown overnight. Cells were then examined under a fluorescent microscope with a GFP filter (upper) and replica-plated onto medium lacking adenine (-Ade) where only [*PSI*$^{+}$] cells can grow. Plates were photographed after incubation. Patches of three independent transformants of [*PIN*$^{+}$] and [*pin*$^{-}$] are shown (lower).

Fig. 6 Heat stress causes transfer of some CREST aggregates from the nucleus to the cytoplasm. CREST partially co-localizes with the EDC3 P-body marker during heat-stress and returns to the nucleus following heat stress. pEDC3-mCh (p2452) transformants of [*PIN*$^{+}$] 74D-694 with integrated *GAL-CREST-EGFP* (L3536) were grown in plasmid selective SRaf(2%) to OD_{600}=0.3 when CREST-EGFP was induced by addition of 2% galactose for 5 hrs. Cells were then stressed for 20 min at 46°C. CREST-EGFP and EDC3-mCh were examined before (30°C), during (46°C) and 3 hrs following (30°C) heat stress.

bioRxiv preprint doi: https://doi.org/10.1101/415927; this version posted September 13, 2018. The copyright holder for this preprint (which was not certified by peer review) is the author/funder. All rights reserved. No reuse allowed without permission.

TABLE 1. YEAST STRAINS USED.

Strains	Description	Reference
74D-694	*MAT***a** *ade1-14 ura3-52 leu2-3,112 trp1-289 his3-200*	[52]
L2910	74D-694 [*psi-*] [*pin-*]	[52]
L1749	74D-694 [*psi-*] [*PIN+*]	[52]
L3536	L1749 *GAL-CREST-EGFP:: LEU2*	This study
L3491	74D-694 [*psi-*] [*PIN+*] *HTB1-mCh::LEU2*	[35]
L3496	[*pin-*] version of L3491	[35]
BY4741	*MAT***a** *his3Δ1 leu2Δ0 met15Δ0 ura3Δ0*	[96]
L3270	BY4741 [*psi-*] [*PIN+*]	[52]
L3269	BY4741 [*psi-*] [*pin-*]	[52]
L3539	BY4741 [*psi-*] [*PIN+*] *pbp1Δ::KanMX4*	[97]
L3570	BY4741 [*psi-*] [*pin-*] *pbp1Δ::KanMX4*	This study
GF513(UCC3537)	*MATa ura3-52 lys2-801 ade2-101 trp1-Δ63 his3-Δ200 leu2-Δ1 URA3-TEL-VII-L ADE2-TEL-V-R*	[58]
L1642	UCC3537 *rad6::LEU2*	[58]

bioRxiv preprint doi: https://doi.org/10.1101/415927; this version posted September 13, 2018. The copyright holder for this preprint (which was not certified by peer review) is the author/funder. All rights reserved. No reuse allowed without permission.

TABLE 2. PLASMIDS USED.

SWL Laboratory Plasmid #	Original Plasmid Name/Description	Reference
p798	pHCA/*GAL4(1–93).ER.VP16*	[98]
p1181	pRS413-*CUP1-SUP35NM-GFP* (*HIS3*)	[60]
p1764	pAG416-*GAL1-ccdB-EGFP* (*CEN*, *URA3*)	Addgene plasmid #14195
p2042	pRS416-Gal-TDP43-YFP (*CEN, URA3*)	Addgene plasmid #27447
p2043	pAG416-*GAL1-FUS-YFP* (*CEN, URA3*)	This study
p2186	pAG413-*GAL-ccdB*	Addgene plasmid #14153
p2228	pBY011-*GAL1-PBP1* (*CEN, URA3*)	[40]
p2229	pBY011-*GAL1* (*CEN, URA3*)	[90]
p2342	p*EGFP-C1-CREST*	[50]
p2370	pDONR-*CREST* without stop codon	This study
p2375	pAG416-*GAL1-CREST-EGFP* (*CEN, URA3*)	This study
p2380	pAG425-*Gal-ccdB-GFP* (2μ, *LEU2*)	Addgene plasmid #14201
p2381	pAG425-*GAL1-CREST-EGFP* (2μ, *LEU2*)	This study
p2387	pAG425-*GAL-ccdB-DsRED* (2μ, *LEU2*)	Addgene plasmid #14369
p2389	pAG425-*GAL1-CREST-DsRED* (2μ, *LEU2*)	This study
p2391	pAG305-*GAL1-CREST-EGFP* (*YIp*, *LEU2*)	This study
p2425	pAG305-*GAL-ccdB-EGFP* (*YIp*, *LEU2*)	Addgene plasmid #14185
p2452	pRP1574, *EDC3-mCh* (*CEN URA3*)	[99]
p2471	pAG423-*GAL1-CREST-YFP* (2μ, *HIS3*)	This study

bioRxiv preprint doi: https://doi.org/10.1101/415927; this version posted September 13, 2018. The copyright holder for this preprint (which was not certified by peer review) is the author/funder. All rights reserved. No reuse allowed without permission.

a

No β-Estradiol | + β-Estradiol

v + pβ-est

CEN GAL-CREST-GFP + v

CEN GAL-CREST-GFP + pβ-est

b

No β-Estradiol | + β-Estradiol

v + pβ-est

2μ GAL-CREST-GFP + v

2μ GAL-CREST-GFP + pβ-est

c

No β-Estradiol | + β-Estradiol

No plasmid integrated

v + v

v + pβ-est

GAL-CREST-GFP Integrated

v

pβ-est

d

No β-Estradiol | + β-Estradiol

[*PIN*$^+$]

CREST + v

CREST + pβ–est

CREST + pβ–est

[*pin*$^-$]

CREST + v

CREST + pβ–est

CREST + pβ–est

bioRxiv preprint doi: https://doi.org/10.1101/415927; this version posted September 13, 2018. The copyright holder for this preprint (which was not certified by peer review) is the author/funder. All rights reserved. No reuse allowed without permission.

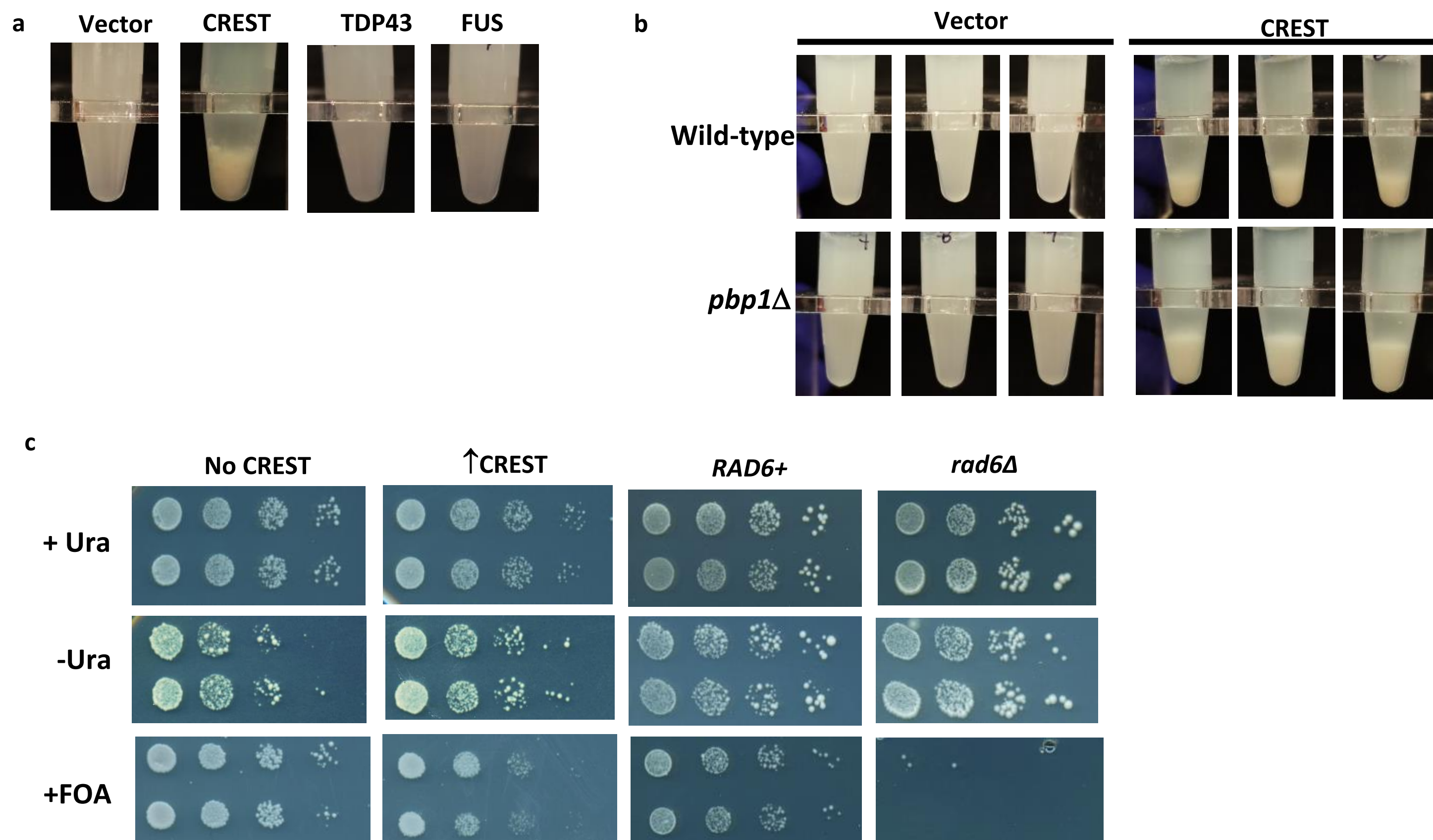

bioRxiv preprint doi: https://doi.org/10.1101/415927; this version posted September 13, 2018. The copyright holder for this preprint (which was not certified by peer review) is the author/funder. All rights reserved. No reuse allowed without permission.

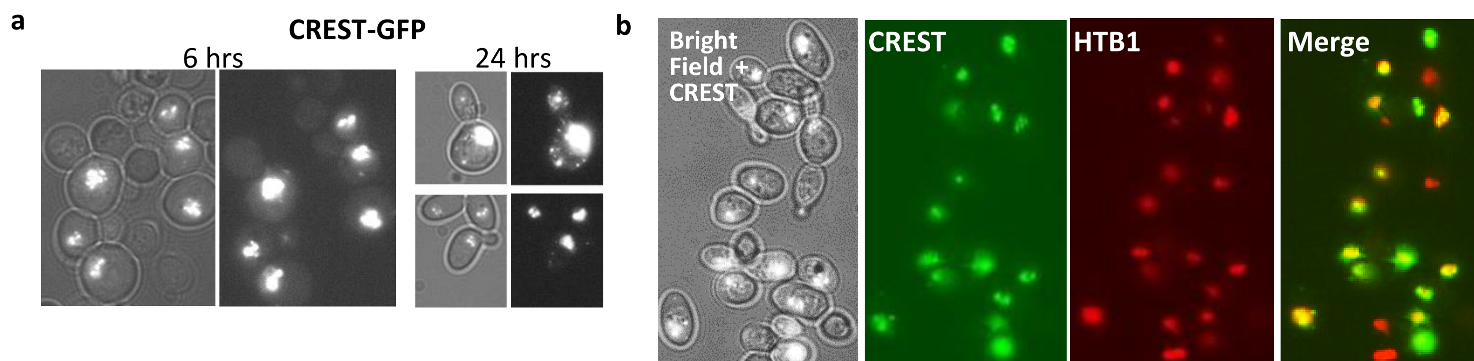

c

TDP43-YFP (Negative Ctr)

FUS-YFP

CREST-YFP

↑PBP1 CREST-YFP

CFP (ThT)

YFP

Merge (CFP and YFP)

mCH (HTB1)

Merge (CFP and mCH)

bioRxiv preprint doi: https://doi.org/10.1101/415927; this version posted September 13, 2018. The copyright holder for this preprint (which was not certified by peer review) is the author/funder. All rights reserved. No reuse allowed without permission.

a

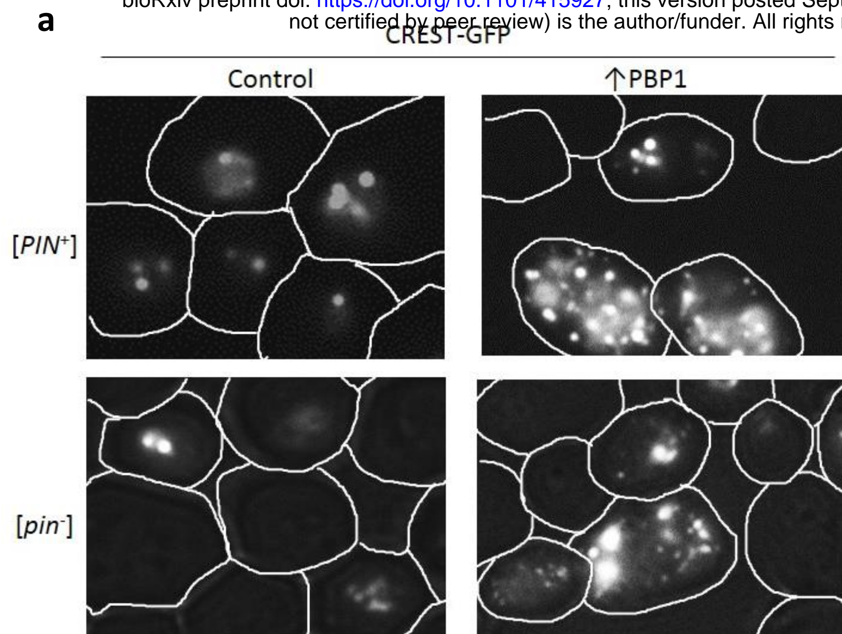

b

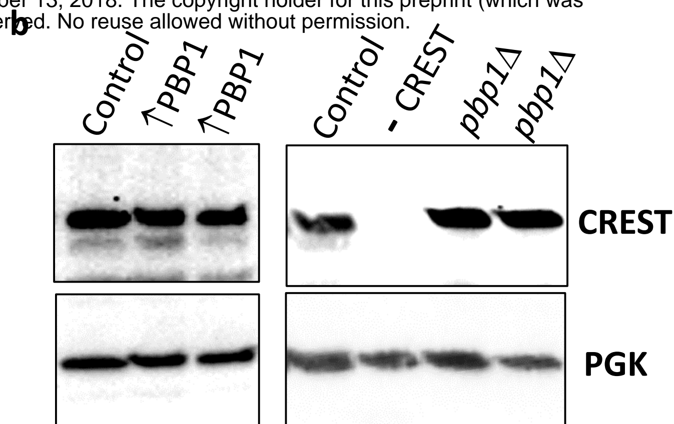

c

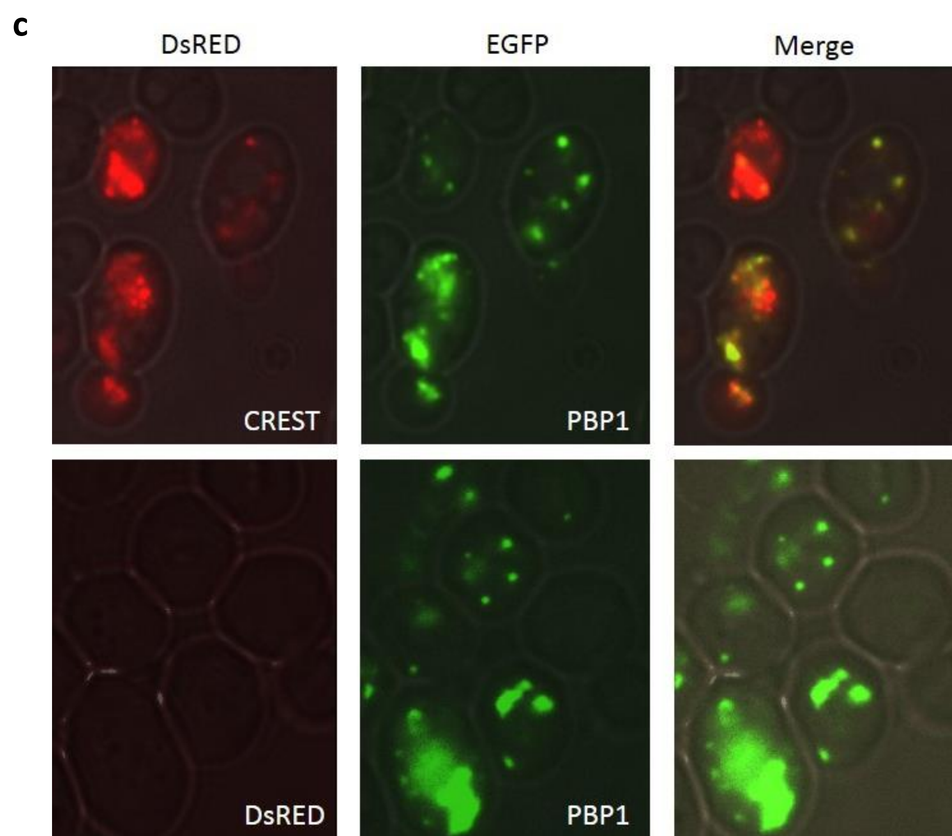

d

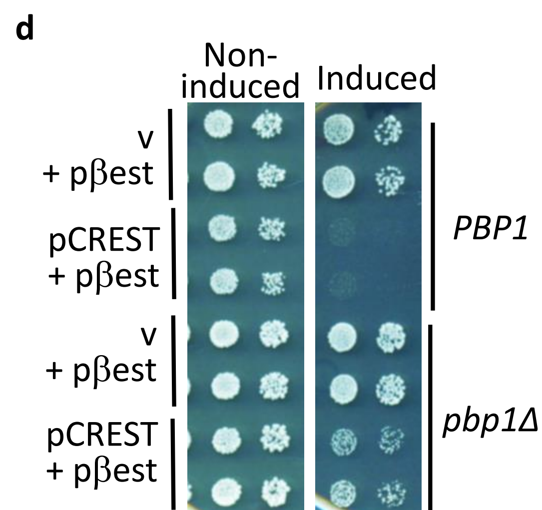

e

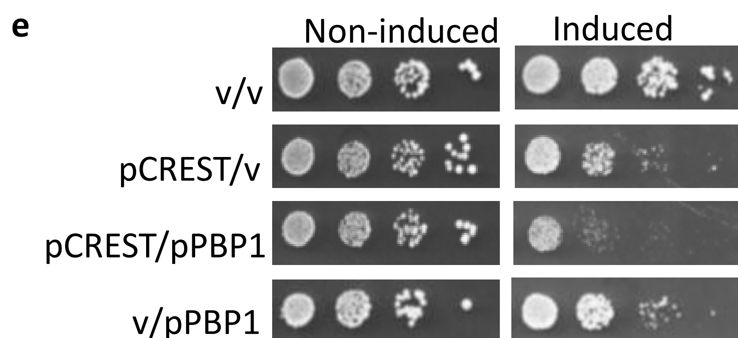

bioRxiv preprint doi: https://doi.org/10.1101/415927; this version posted September 13, 2018. The copyright holder for this preprint (which was not certified by peer review) is the author/funder. All rights reserved. No reuse allowed without permission.

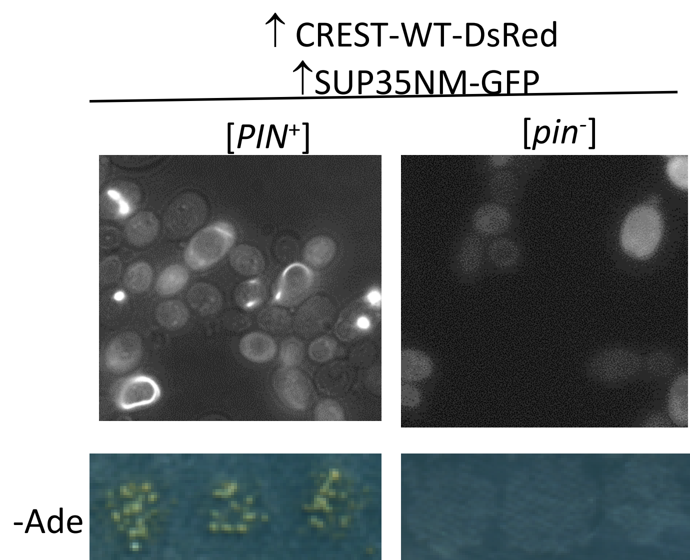

bioRxiv preprint doi: https://doi.org/10.1101/415927; this version posted September 13, 2018. The copyright holder for this preprint (which was not certified by peer review) is the author/funder. All rights reserved. No reuse allowed without permission.